Journal of Engineering Research and Reports

20(7): 56-67, 2021; Article no.JERR.68313
ISSN: 2582-2926

Influence of Fiber Properties on Harmonic and Intermodulation Distortions of Semiconductor Lasers

Moustafa Ahmed[1*], Yas Al-Hadeethi[1] and Ghodran Alghamdi[1]

[1]Department of Physics, Faculty of Science, King Abdulaziz University, 80203 Jeddah 21589, Saudi Arabia.

Authors' contributions

This work was carried out in collaboration among all authors. Author MA designed the study, wrote the protocol and wrote the first draft of the manuscript. Authors YAl-H and GA managed the literature searches and the system design. Author GA performed the simulations. All authors read and approved the final manuscript.

Article Information

DOI: 10.9734/JERR/2021/v20i717342
Editor(s):
(1) Dr. P. Elangovan, SRM TRP Engineering College, India.
Reviewers:
(1) Zunuwanas Bi Mohamad, Politeknik Bagan Datuk, Malaysia.
(2) Mohammed Rasheed, University of Technology, Iraq.
(3) S. Ramabalan, EGS Pillay Engineering College, India.
Complete Peer review History: http://www.sdiarticle4.com/review-history/68313

Original Research Article

Received 05 March 2021
Accepted 15 May 2021
Published 18 May 2021

ABSTRACT

This paper introduces modeling and simulation of the harmonic and intermodulation distortions of semiconductor laser radiating an optical fiber link. The study is based on the rate equation model of semiconductor lasers excited by injection current with two sinusoidal tones separated by a radio frequency. The modulated laser signal is modeled in both the time and frequency domains. The laser signal distortions include the 2nd and 3rd harmonic distortion (2HD and 3HD), and the third-order intermodulation distortion IMD3. The laser is assumed to be modulated around its relaxation frequency. Influence of the modulation depth on the signal distortion is investigated when the laser is free running and when it is radiating a fiber link. In the latter case, influences of the attenuation and chromatic dispersion on the signal dispersion are elucidated when the fiber length increases up to 10 km. The results show that the fiber attenuation does not affect the signal distortion, whereas the chromatic dispersion affects both the harmonic distortions and intermodulation distortion. Sending the laser signal down an optical fiber of length ~ 5km can help in minimizing 2HD which is the dominant harmonic distortion of the modulated signal. This range of optical fiber is also characterized with intermodulation distortion less than 0dBc.

**Corresponding author: Email: mostafa.farghal@mu.edu.eg;*

Keywords: Current modulation; harmonic distortion; intermodulation distortion; fiber dispersion; semiconductor laser.

1. INTRODUCTION

Fiber-optic links are widely used in various areas of science and technology. Although digital fiber optic systems are known to give superior performance, the present cost of high-speed electronics and the continual increase in the speed of direct modulated semiconductor laser have given analog fiber links much attention. Examples of optical systems that employ high speed fiber links include cable television (CATV) systems and radio over fiber (RoF) networks [1-4]. The bandwidth of conventional semiconductor laser is several GHz [5], and was increased to more than 20 GHz with the invention of multiple quantum well lasers [6]. With suitably chosen components of the fiber link, the link performance is mostly dominated by laser nonlinearities. Nonlinearities in laser diodes root to both nonlinearity in the light current characteristic and intrinsic nonlinearity due to laser resonance. The former is induced by device imperfections, such as leakage current and dominates at low radio frequencies (MHz), therefore, it is diminished in state of art lasers due to improvement in fabrication technique. The nonlinearities associated with laser resonance are associated with spatial hole burning, gain suppression [7,8], and produce higher harmonics that manifest themselves in generation of higher-order harmonic distortions (HDs) that are not presented in the original signal. [9-11]. Previous reports showed that the signal distortions are enhanced around the relaxation frequency of the laser [12-14].

In analog optical fiber applications and for the purpose of increasing the transmission speed, the laser is modulated by two signals with adjacent frequencies. This type of two-tone modulation happens to results in intermodulation distortions (IMDs) in additions to HDs [15-19]. IMDs have two types; namely, IMD2 and IMD3, which describe the spectral power at the sum and difference between the modulation two-tone frequencies, respectively. These intermodulation components are located very close to the modulation frequencies and can fall within the narrow transmission band of an optical link [15-19].

The performance of fiber links depends largely on the non-linear properties of the system and the produced distortions [9,10]. For these systems, it is useful to have an a priori knowledge of the distortion produced by the directly modulated laser diode. Therefore, estimation and prediction of these products are therefore of great importance. Also, it is essential to minimize the signal distortions in order to increase the transmitted information capacity in analog fiber links [20]. Intensive research works were reported on investigating HDs and IMD3 and determining the corresponding spurious free spectral range (SFDR) of the laser [9,10,13,15-21]. Mendis et al. [22] showed that such intermodulation distortions are lowered by large gain compression. Krehlik [23] reported that frequency chirping of directly modulated semiconductor laser interacts with chromatic dispersion of optical fibers and causes distortions of the signal travelling along the optical fiber. Bakry and Ahmed [18] introduced numerical simulations on the signal distortions of MQW lasers under two-tone modulation. They reported that IMD3 increases with the increase of the modulation frequency, showing a broad peak around the resonance relaxation frequency with values ranging between -55 and -10 dBc [18]. Also, IMD3 was found to increase with the increase of the modulation index [18].

This paper introduces modeling and simulation of the signal distortions, including HDs and IMD3 of semiconductor lasers under two-tone modulation when the laser is injected near and far above the threshold level. Influence of the fiber length of a fiber link that uses the directly modulated laser on the signal distortions is examined. The main aim is to explore the optimum ranges of the modulation index and fiber length that correspond to laser signal with minimum HDs and IMD3. The study is based on the rate equation model of semiconductor lasers excited by injection current with two sinusoidal tones separated by a radio frequency as low as 10 MHz. The modulated waveform and the associated frequency spectrum of the signal are simulated. It is shown that IMD3 of the free running laser is the highest distortion type up to modulation depth of 0.4, and then the 2nd-order harmonic distortion, 2HD, dominates the signal distortion. The fiber attenuation works to decrease the power of the laser signal uniformly, and both HDs and IMD3 do not change. The chromatic dispersion of the fiber changes both HDs and IMD3 of the laser signal when propagates down the optical fiber. Fiber length of

5 km is found to minimize 2HD which is the dominant harmonic distortion of the modulated signal. Also, fibers shorter than 5km are characterized with intermodulation distortion of IMD3 < 0dBc over the entire range of *m*.

2. METHODOLOGY

The dynamic behavior of the semiconductor laser under current modulation is analyzed using the rate equation model of single-mode lasers. These rate equations describe the time evolution of the photon density *S(t)* and injected carrier density *N(t)* are given by [24]

$$\frac{dN}{dt} = \frac{I(t)}{eV} - \frac{N}{\tau_e} - G(N,S) \quad (1)$$

$$\frac{dS}{dt} = \Gamma G(N,S)S - \frac{S}{\tau_p} + R_{sp} \quad (2)$$

where *G* is the optical gain and is described by the following nonlinear form

$$G(N,S) = g_0 \frac{N-N_g}{1+\varepsilon S} \quad (3)$$

where g_0 is the gain slope constant, ε is the gain compression factor, N_g is the carrier density at transparency, R_{sp} is rate of inclusion of spontaneous emission into the lasing mode, Γ is the mode confinement factor, *V* is the active layer volume, τ_p is the photon lifetime

In the two-tone sinusoidal modulation, the injection current *I(t)* is given by the following form:

$$I(t) = I_b + I_m[\sin(2\pi f_{m1}t) + \sin(2\pi f_{m2}t)] \quad (4)$$

where I_b is the bias current and I_m is the modulation current, which defines the modulation depth $m=I_m/I_b$. In the above equation, f_{m1} represents the modulation frequency of the first tone, while the second tone frequency is defined in terms of the frequency spacing Δf_m as $f_{m2} = f_{m1} + \Delta f_m$. The time variation for the optical power *P(t)* is determined from the photon density *S(t)* via the relationship:

$$P(t) = \frac{\eta_0 h\nu}{2\Gamma\tau_p} VS(t) \quad (5)$$

where η_0 is the differential quantum efficiency, ν is the optical frequency, and *h* is the Planck's constant. The frequency spectrum of the modulated signal $P_f(f)$ over time period *T* are determined from the signal power *P(t)* as

$$P_f(f) = \frac{1}{T}\left|\int_0^T P(\tau)e^{-j2\pi f\tau}d\tau\right| \quad (6)$$

where *f* is the noise Fourier frequency.

Table 1. Typical values of the DFB 1.55μm-InGaAsP laser and PIN photodiode parameters [24]

Symbol	Definition	Value
Laser Parameters		
λ	Wavelength	1.55 □m
V	Active layer volume	1.5×10^{-16} m^3
v_g	Group velocity	8.5×10^{9} cm/s
η_0	Quantum efficiency	0.4
a_0	Differential gain coefficient	2.5×10^{-20} m^2
N_g	Carrier density at transparency	1×10^{24} m^{-3}
α	Linewidth enhancement factor	5
Γ	Mode confinement	0.4
τ_N	Carrier lifetime	1×10^{-9} s
τ_π	Photon lifetime	3×10^{-12} s
R_{sp}	Rate of spontaneous emission	3×10^{-5}
ε	Gain compression coefficient	1×10^{-23} m^3
Optical fiber		
a_F	Attenuation coefficient	0.2 dB/km
D	Dispersion parameter	16.75 ps/nm/km
S_F	Dispersion slope	0.075 ps/nm^2/km
PIN Photodetector		
R	Responsivity	1 A/W

The above theoretical model is simulated by using the powerful software "Optisystem" (software for design and simulation of optical communication system). The time trajectories of the laser power *P(t)* are evaluated over sufficient long time expending more than 256 cycles of period $T=1/f_{m1}$. The calculations are applied to an InGaAsP DFB laser emitting with λ=1.55 μm using the parametric values given in table 1 [24]. The calculated value of the threshold current is I_{th} = 33.45 mA. The bias current is set to be far above the threshold level, $I = 2.0I_{th}$. The power spectrum P_f in Eq. (6) calculated by using the FFT of *P(t)* as [25].

$$P_f(f) = \sqrt{\frac{\Delta t}{T}} |FFT[P(t)]| \tag{7}$$

In this calculation, the longer half of the time trajectory of S(t) is considered, which ascertains that the transients are discarded and the output is stabilized.

The laser signal is transmitted down by a standard single-mode fiber of length L_f, attenuation coefficient α_f and dispersion *D*. When the optical field maintains its polarization along the fiber length, the pulse-envelop amplitude of the electric component of the optical field is assumed to vary slowly, $E=E(z, \tau)$. The evolution of $E(z,\tau)$ along the fiber can be described by a single nonlinear Schrödinger equation of the form [26,27]:

$$\frac{\partial E}{\partial z} + \alpha_F E + i\beta_2 \omega_0 \frac{\partial^2 E}{\partial \tau^2} = 0 \tag{8}$$

where a frame moving at the group velocity v_g is assumed with $\tau = t - z/v_g \equiv t - \beta_1 z$ being the reduced time. β_2 is the group velocity dispersion GVD, and ω_0 is the reference frequency of the signal. The first in the above equation takes into account the slow changes of the optical field along the fiber length. The second term takes into account the linear losses of the optical fiber. The third term represents the first-order group velocity dispersion, which is responsible for the pulse broadening. The following relations are used internally to convert between them and the commonly used wavelength domain parameters *D* (dispersion) and S_F (dispersion slope).

$$D = -\frac{2\pi c}{\lambda^2}\beta_2 \qquad S_F = \frac{\partial D}{\partial \lambda} \tag{9}$$

The receiver detects the laser signal and converts it into an electrical signal by a photodiode detector diode of responsivity *R*. Both the shot and thermal noises are ignored. The values of the attenuation coefficient α_F, and dispersion *D*, and dispersion slope S_F of this fiber for λ=1.55μm are also listed in the Table 1.

Figure plots a scheme of present design of the modulated laser signal propagation and detection using the Optisystem software.

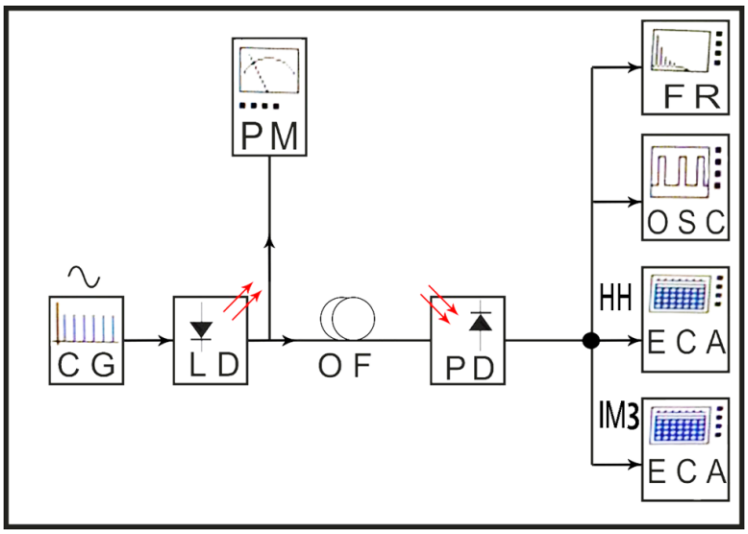

Fig.1. Scheme of the designed system of laser signal modulation, propagation down the optical fiber and detection along with harmonic and intermodulation evaluation by Optisystem; (C.G: carrier generator, LD: laser diode, PM: power meter, OP: optical fiber, PD: photodetector, RF: spectrum analyzer, OSC: oscilloscope, ECA: electric carrier analyzer)

3. RESULTS AND DISCUSSIONS

3.1 Two-Tone Modulation Signal

An example of the waveform of the two-tone modulated laser signal is plotted in Fig. 2 when the modulation frequency is set to be the relaxation frequency of the laser f_r. This relaxation frequency is evaluated from the Optisystem as the peak value of the small-signal intensity modulation response. The calculated values is f_r =5.25 GHz when the bias current is set to be $I_b = 2I_{th}$. The results in the figure correspond to modulation depth of m = 0.2 and frequency separation of Δf_m = 10 MHz. The modulated signal exhibits slow (envelope) variation with the intermodulation frequency separation Δf_m = 10 MHz, and fine variation with the fundamental frequency f_{m1} as shown in insets (a) and (b). These onsets indicate that the signal deviates from the sinusoidal character of the modulating current in equation (4), because of the deep modulation with m = 0.2 which results signal clipping and pulse generation around crests of the envelope, as seen in inset (b). These results indicate higher signal distortion as reported by Bakry and Ahmed [18].

The Fourier frequency spectrum of the modulated signal in Fig. 2 is plotted in Fig. 3. The spectrum exhibits pronounced peaks around the fundamental frequencies f_{m1} = 5.25 GHz and f_{m2} = 5.26 GHz and their higher harmonics. The remarkable peaks at the harmonic frequencies indicate higher harmonic distortions. The characterizing 2HD and 3HD is calculated as

$$2\mathrm{HD}\,(\mathrm{dBc}) = 20\log_{10}\frac{a_{2f_{m1}}}{a_{f_{m1}}} \tag{10}$$

$$3\mathrm{HD}\,(\mathrm{dBc}) = 20\log_{10}\frac{a_{3f_{m1}}}{a_{f_{m1}}} \tag{11}$$

where a_{fm1}, a_{2fm1} and a_{3fm1} are the peak powers at the modulation frequency f_{m1}, second-order harmonic $2f_{m1}$ and third-order harmonic $3f_{m1}$ In this case, 2HD = -4.45 dBc and 3HD = -13.55 dBc.

The frequency variations of the signal around the fundamental peak are zoomed in the inset to show the third-order intermodulation (IM2 and IM3) products. The Inset shows appearance of the IM2 components (f_{m1} + f_{m2}) and IM3 components at ($2f_{m1}$ - f_{m2} = f_{m1} -Δf_m) and (f_{m2} +Δf_m), respectively, in addition to weaker components at lower and higher k-components at f_{m1} -$k\Delta f_m$ and f_{m2} +$k\Delta f_m$. The most important intermodulation product is IM3 [18], and the associated third-order intermodulation distortion IMD3 is defined as the ratio (in dBc), of the amplitude of IM3 components to a_{fm1} as [18],

$$\mathrm{IMD3(dBc)} = 20\log_{10}\frac{a_{f_{m1}-\Delta f}}{a_{f_{m1}}} \tag{12}$$

The present value of this intermodulation distortion is IMD3 = -12.7 dBc, which is still smaller than the critical level of -5dBc that corresponds to crosstalk of the intermodulation component.

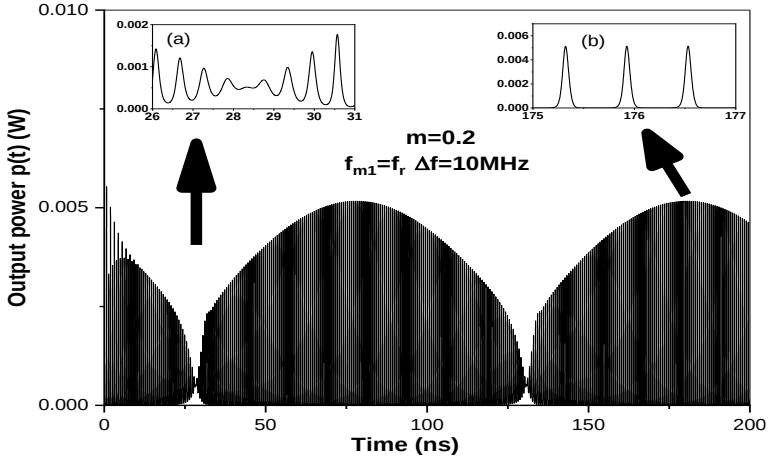

Fig. 2. The waveform of the two-tone modulated laser diode when f_{m1} = 5.25 GHz, Δf_m= 10 MHz and m = 0.2. The frequency of the envelope is Δf_m while the frequency of the fine variation corresponds to f_{m1}.

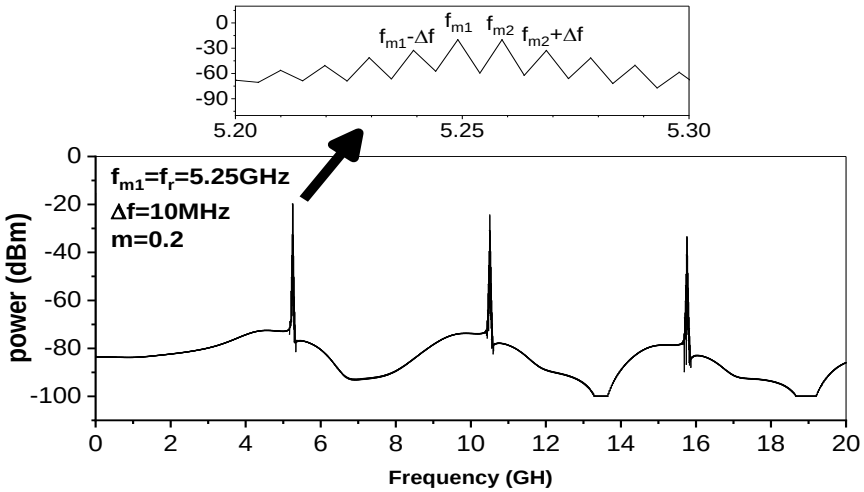

Fig. 3. The Fourier frequency spectrum of the two-tone modulated laser signal when f_{m1} = 5.25 GHz, Δf_m= 10 MHz and m = 0.2. The figure displays the 2nd and 3rd order harmonics of the signal. The intermodulation products around f_{m1} are seen in the inset

3.2 Signal Distortions

3.2.1 Modulation of the free-running laser

Fig. 6 illustrates influence of the modulation index m on the two-tone modulation performance of the investigated laser diode. Fig. 4(a) plots variations of the power of the fundamental component at $f = f_{ma}$, power of the second order harmonic ($f = 2f_{ma}$), power of the third-order harmonic ($f = 3f_{ma}$), and power of the third-order intermodulation component (IM3) with m, while Fig. 4(b) plots the corresponding variations of the induced HDs (2HD and 3HD) and IMD3. Fig. 4(a) shows that the power (in logarithmic scale) of the fundamental component and the 2nd and 3rd order harmonics increase in general with the increase of m. IM3 ranges between –41 dBm and –24 dBm. Up to m = 0.4, IM3 is higher than the higher harmonics, while around m ~ 0.9, both IM3 and the second harmonic attain almost similar powers. These results manifest in the corresponding variations of the signal distortions shown in Fig. 5, which indicates that the intermodulation distortion IMD3 is the highest distortion type up to m = 0.4, and then the 2nd-order harmonic distortion, 2HD, dominates the signal distortion. The 3rd-order harmonic distortion is the lowest distortion, ranging as 3HD = –54 ~ –35 dBc. The intermodulation distortion ranges between IMD3 = –18 ~ –3 dBc.

These results on the intermodulation product and distortion can be understood from Fig 5, which plots the modulated laser signal and the corresponding power spectrum around the modulation frequencies f_{m1} and f_{m2} when m = 0.01, 0.2, 0.5, 0.7 and 0.9. Fig 5(a) shows that when m = 0.01, the signal is almost sinusoidal and the IM3 component in Fig 5(a1) is very weak, which then corresponds to very weak distortion IMD3. When m increases, Figs 5(b) – (e) show that the high-frequency oscillations (at f_{m1}) are clipped and so does the lower envelope of oscillating frequency f_{m2} - f_{m1}. The clipping of the signal increases with the increase of m due to the gain switching mechanism associated with moving the lower cycles of the modulating current below the threshold current I_{th} [25,28]. The signal distortion is clearer in the envelope of the modulated signal in Figs 5(c) – (e). Figs 5(c1) – (e1) shows that little increase in the fundamental components at f_{m1} and f_{m2} as well as in the intermodulation products around them, which manifests as the little increase of distortion IMD3 in Fig. 4(b).

3.2.2 Influence of fiber attenuation on signal distortions

In order to study influence of the optical fiber properties; namely, attenuation and chromatic dispersion, on the modulated laser signal, the signal is assumed to be coupled into an optical fiber of length L_f, attenuation α and dispersion parameter D.

Influence of fiber attenuation on laser modulation, the fiber dispersion (D = 0) is ignored, and both the fiber length L_f and

modulation index *m* are varied, and then the laser signal and its power Fourier spectrum are recorded. Fig. 6(a) plots variation of the signal power at the fundamental frequency f_{m1}, the 2nd and 3rd-order harmonics and the intermodulation product IM3 with the fiber length L_f when *m* = 0.5. The figure indicates that the power (in logarithmic scale) at the characteristics frequencies decrease linearly with the increase of the fiber length L_f. These results agree with the Beer's law that relates the fiber attenuation coefficient α (in dB/km), length L_f (in km) with the relative power ($P=P_{out}/P_{in}$) as

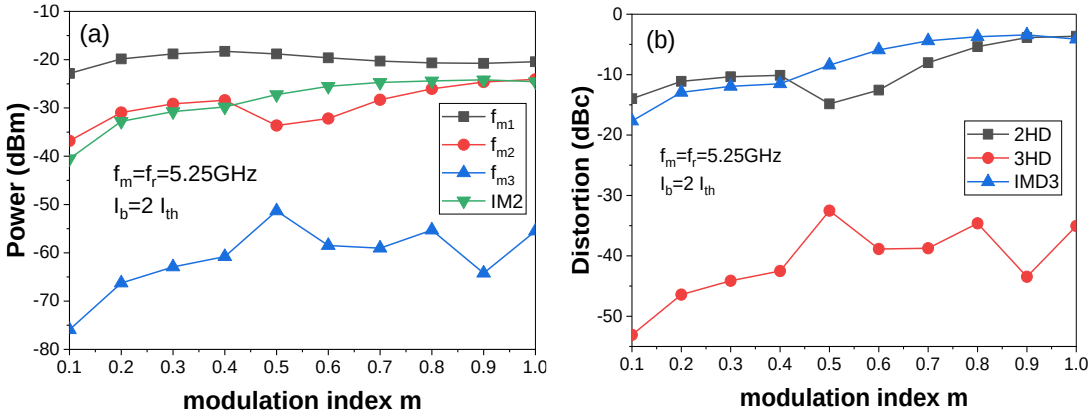

Fig. 4. Influence of the modulation index *m* on (a) power of the fundamental component, higher harmonics and IM3, and (b) distortions 2HD, 3HD and IMD3 when $I = 2I_{th}$ and $f_m = f_r = 5.25$ GHz

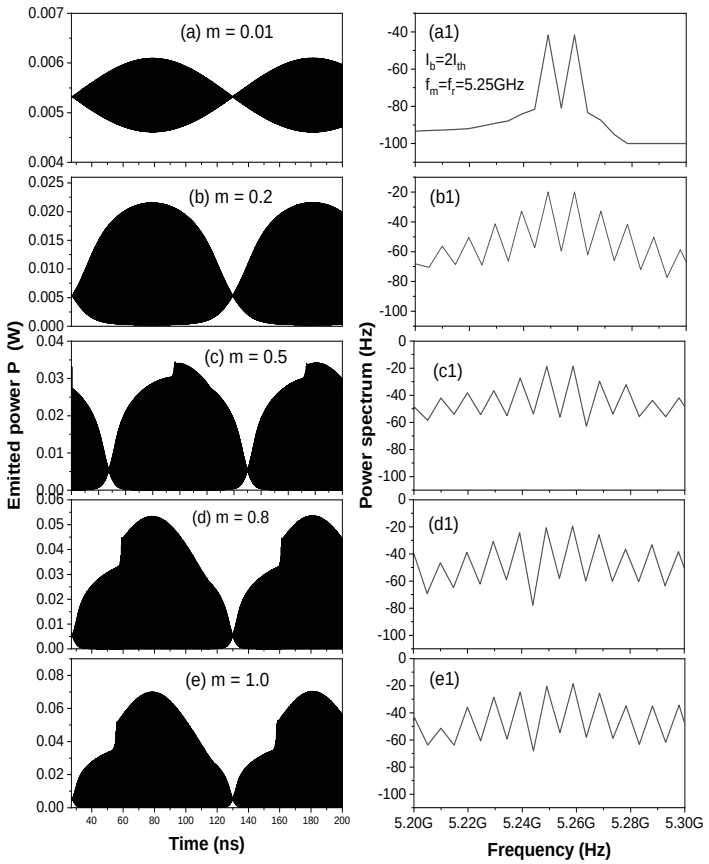

Fig. 5. Two-tone modulation results: (a) – (e) modulated signals, and (a1) – (e1) Fourier power spectra when *m* = 0.01, 0.2, 0.5, 0.7 and 0.9, respectively

$$L\,(\mathrm{km}) = \frac{1}{\alpha(\mathrm{dBm/km})} log_{10}(P) \qquad (13)$$

This linear variation of the laser modulation frequency components indicates no variations in the signal distortions, either HDs or IMD3. This is clear in Fig. 6(b), which then confirms that the fiber attenuation does not change the signal distortion.

3.2.3 Influence of fiber chromatic dispersion on signal distortions

In this case, the fiber attenuation (= 0) is ignored, both the fiber length L_f and modulation index m are varied and then the laser signal and its power Fourier spectrum are recorded. The influence of the chromatic dispersion on the modulated signal and spectrum is illustrated in Fig. 7 at different lengths L_f of the optical fiber when m = 0.2. Figs 7(a) – (e) show that the increase of the fiber length causes reduction in the signal amplitude, which is then attributed due to the chromatic dispersion of the fiber. It has been recognized the fiber dispersion works to broaden the signal duration at expense of the signal power, and this effect becomes significant in long fibers [5]. Figs 7(a1) – (e1), which plot the corresponding spectrum around the two modulation frequencies f_{m1} and f_{m2}, and indicate decrease in the amplitudes of frequency components.

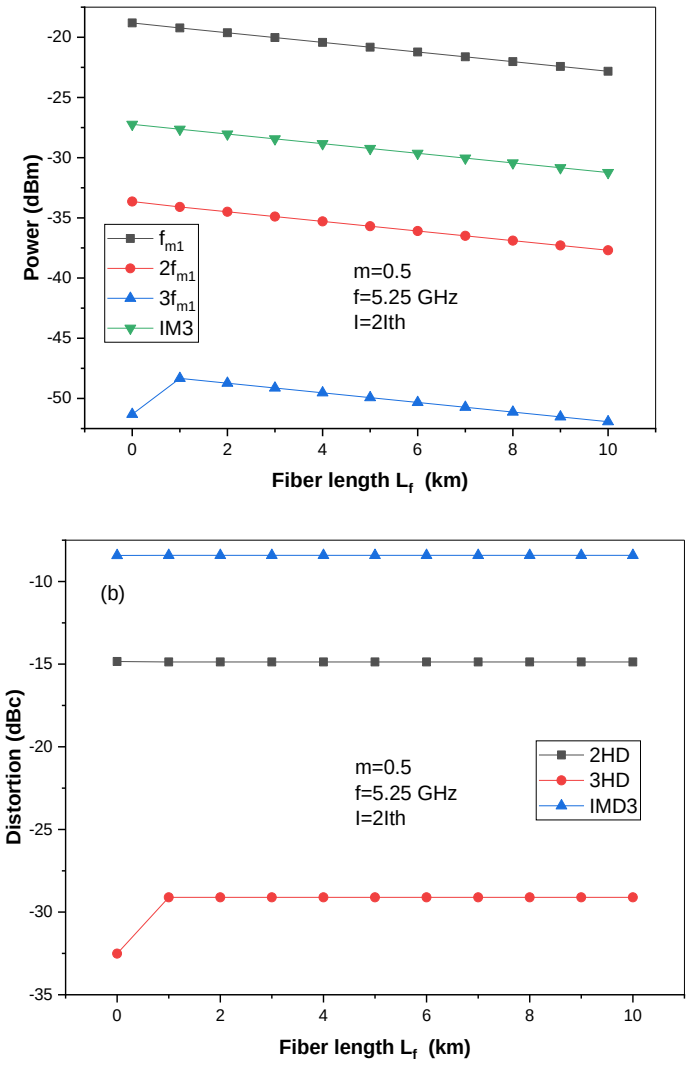

Fig. 6. Influence of fiber length L_f using attenuation only and modulation index m on: (a) power of frequency component around f_m, $2f_m$, $3f_m$ and $f_{m1} + \Delta f_m$, and (b) distortions 2HD, 3HD and IMD3

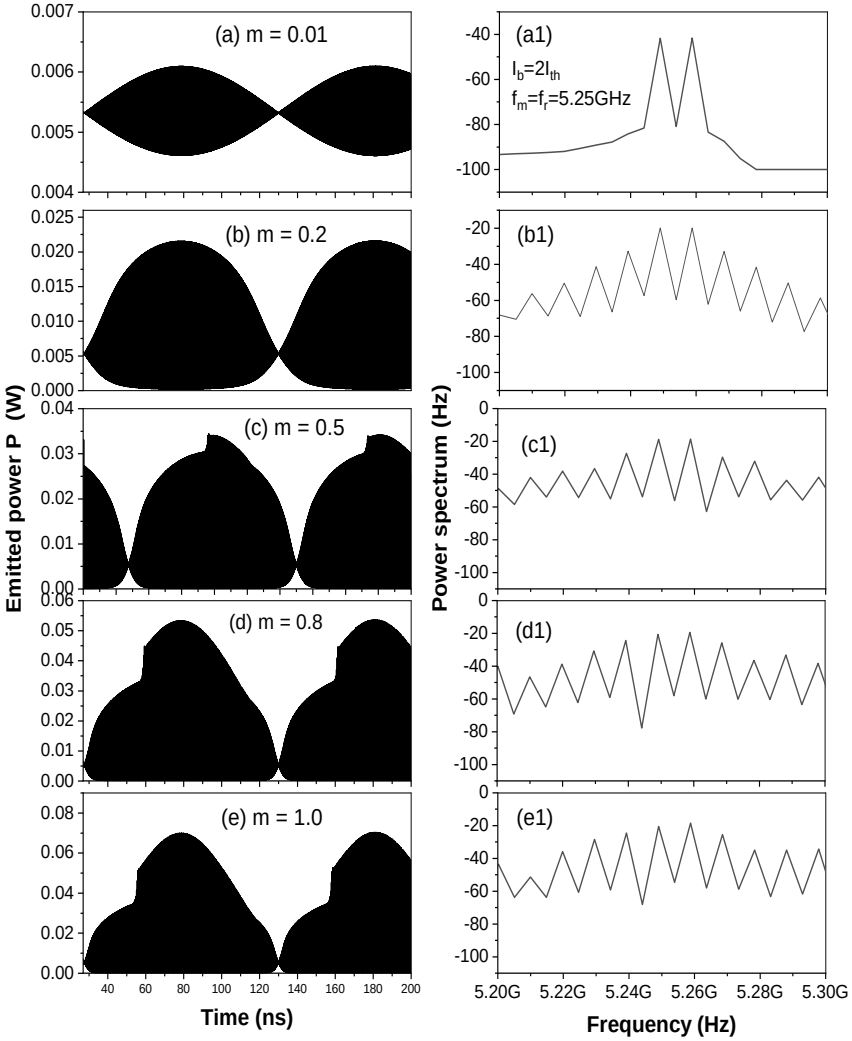

Fig. 7. Two-tone modulation results: (a) – (e) modulated signals, and (a1) – (e1) Fourier power spectra when L_f = 1, 3, 5, 7 and 9 km, respectively using m = 0.2

Quantitative analysis of the power of these frequency components are given in Fig. 8, which plots the intermodulation distortion IMD3 as a function of the fiber length L_f over the relevant range of the modulation index m = 0.1 ~ 1.0. The figures shows that IMD3 increases with the increase of L_f, and the range of this increase gets wider with the increase of m; this range is -18 ~ -15 dBm when m = 0.1 and becomes -5 ~ +6 dBc when m = 1.0. The increase in the depth of modulation m results also in enhancing the intermodulation distortion IMD3. As the figure shows, IMD3 happens to be larger than 0 dBc, which indicates that the intermodulation product IM3 exceeds the power at the fundamental frequency f_{m1}. This level occurs when the fiber length L_f exceeds 5 and m > 0.5. As a numeric example on influence of m, IMD3 ranges between -18 and -15 dBc over the relevant range of L_f when m = 0.1, which increases to range between -4 and +6 dBc when m = 0.9.

The corresponding influence of the fiber length L_f and modulation depth m on the higher-harmonic distortions 2HD and 3HD are plotted in Figs 9(a) and (b), respectively. The figures show that 2HD is changing over a wide range of (–50 ~ 5 dBc) whereas the range of 3HD is as low as below –30dBc over the relevant range of L_f. The figures show also that, in general, 2HD and 3HD exhibit similar behavior to IMD3 that they increase with the increase of the modulation index m. However Fig 9(a) indicates an interesting behavior that 2HD decreases with the increase of the fiber length L_f, show a minimum around L_f = 5km, and then increases again. The values of 2HD

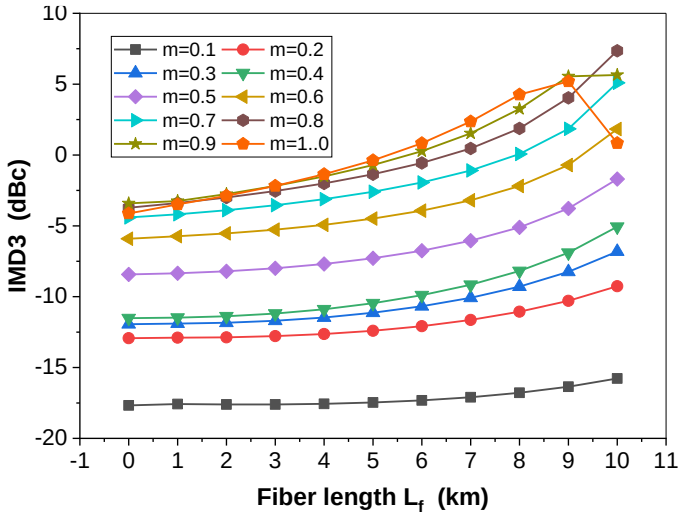

Fig. 8. Influence of fiber length L_f using chromatic dispersion only and modulation index *m* on IMD3

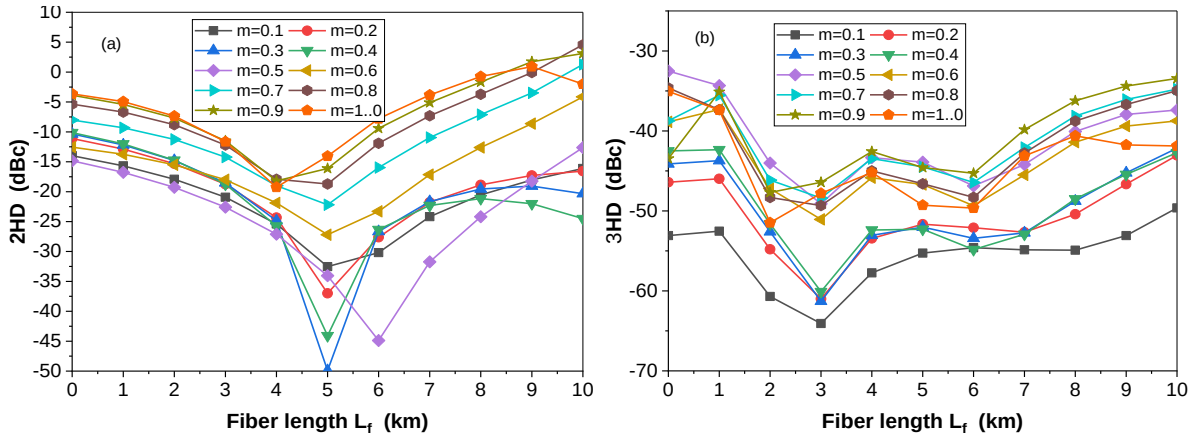

Fig. 9. Influence of fiber length L_f using chromatic dispersion only and modulation index *m* on (a) 2HD and (b) 3HD

exceeds the zero-level when L_f >8 km and *m* = 0.8 and 0.9. Therefore, it can be concluded that sending the laser signal down an optical fiber of length L_f ~ 5km can help in minimizing 2HD which is the dominant harmonic distortion of the modulated signal. By re-checking Fig 8, it could be noticed that the range of L_f ≤ 5km is characterized with intermodulation distortion of IMD3 < 0 over the entire range of *m*.

4. CONCLUSION

Modeling and simulation of the harmonic and intermodulation distortions of semiconductor laser oscillating in single mode and radiating an optical fiber link at wavelength of 1.55 □m were introduced. The laser was assumed to be directly modulated with two tones with frequencies comparable to the relaxation frequency and separated with a frequency interval as short as 10 MHz. The laser signal was modeled in terms of the waveform of the modulated signal and the corresponding Fourier frequency spectrum. The influence of the modulation depth *m* on the signal distortion of the free running laser was explored, and the impacts of the attenuation and chromatic dispersion of the optical fiber on these results were investigated. Basing on the obtained results, the following conclusions are itemized as follows:

1. The intermodulation distortion IMD3 is the highest distortion type up to m = 0.4, and then the 2nd-order harmonic distortion, 2HD, dominates the signal distortion. The 3rd-order harmonic distortion is the lowest

distortion, ranging as 3HD = –54 ~ –32 dBc. The intermodulation distortion ranges between IMD3 = –18 ~ –3 dBc.

2. The increase in the modulation depth m results in clipping of the high-frequency oscillations (at fm1) due to the gain switching mechanism associated with decrease of the lower cycles of the modulating current below the threshold current. This effect is associated with little increase in intermodulation products distortion IMD3.
3. The fiber attenuation works to decrease the power of the laser signal uniformly according to Beer's law, which manifests as equal drop of the Fourier frequency spectrum of the signal. Therefore, the fiber attenuation does not change the signal distortion.
4. The chromatic dispersion of the fiber changes both the harmonic distortions and intermodulation distortion of the laser signal when propagates down the optical fiber. Sending the laser signal down an optical fiber of length Lf ~ 5km can help in minimizing 2HD which is the dominant harmonic distortion of the modulated signal. Also, the range of Lf ≤ 5km is characterized with intermodulation distortion of IMD3 less than the 0dBc level over the entire range of m.

COMPETING INTERESTS

Authors have declared that no competing interests exist.

REFERENCES

1. Darcie TE, Bodeep GE. Lightwave subcarrier CATV transmission systems. J. IEEE Trans. Microwave Theory Techn. 1990;38:524-533.
2. Lipson J, Chainuluupadhyayula L, Yuanhuang S, EEC HB, Roxlo EJ, Flynn PM, Nitzsche CJ, Mcgrath GL. Fenderson, Schaefer MS. High-fidelity light wave transmission of multiple am-VSB NTSC signals. J. IEEE Trans. Microwave Theory Techn. 1990;38:483-493.
3. Brendel F. Millimeter-wave radio-over-fiber links based on mode-locked laser diodes, Karlsruhe: KIT Sci. Pub; 2003.
4. Blauvelt H. Semiconductor lasers for analog applications. Proc. 39th Ann. Meet. IEEE Laser Electro-Optic. Soc. 1993;639-640.
5. Agrawal GP. Fiber-optic communication systems. Wiley J, Sons Inc., New York; 2002.
6. Sato K, Kuwahar S, Miyamoto Y. Chirp characteristics of 40-Gb/s directly modulated distributed-feedback laser diodes. J. Lightwave Technol. 2005;23:3790-3797.
7. Odermatt S, Witzigmann B, Schmithusen B. Harmonic balance analysis for semiconductor lasers under large-signal modulation. J. Opt. and Quan. Elect. 2006;38:1039–1044,.
8. Morthier G, Vankwikelberge P. Handbook of distributed feedback laser diodes. Boston, MA: Artech House;1997.
9. Lau KY, Yariv A. Intermodulation distortion in a directly modulated semiconductor injection laser. J. Appl. Phys. Lett. 1984;45:1034–1036.
10. Jung HD, Han SK. Nonlinear distortion suppression in directly modulated dfb-ld by dual- parallel modulation. J. IEEE Phot. Techn. 2002;14:980-983.
11. Digital communication analyzer (DCA), measure relative intensity noise (RIN). Product note, Agilent Technologies. 2008;86100-7.
12. Bakry A, Ahmed M. Mode Oscillation and Signal Distortion of Modulated Long-Wavelength Semiconductor Lasers. *Opt. laser Techn.* 2013;50:134-140.
13. Westbergh P, Soderberg E, Gustavsson JS, Larsson A, Zhang Z, Berggtren J, Hammer M, Noise, distortion and dynamic range of single mode 1.3 μm InGaAs vertical cavity surface emitting lasers for radio-over-fiber links. IET Optoelectron. 2008;2:88-95.
14. Intermodulation Distortion (IMD) Measurements using the 37300 series vector Network Analyzer. Application Note /GIP-G, Anritsu; 2000.
15. Morton PA, Ormondroyd RF, Bowers JE, Demokan MS. Large-signal harmonic and intermodulation distortions in wide-bandwidth GaInAsP semiconductor lasers. IEEE J. Quantum Electron. 1989;25;1559–1567,.
16. Mahmoud A, Mahmoud SWZ, Ahmed M. Simulation of noise and nonlinear distortions of semiconductor lasers under analog modulation for use in CATV systems. Intl. J. Numer. Model. 2015;29:280-290.
17. Gustavsson JS, Haglund Å, Carlsson C, Bengtsson J, Larsson A. Harmonic and

Intermodulation Distortion in Oxide-Confined Vertical-Cavity Surface-Emitting Lasers. IEEE J. Quantum Electron. 2003;39:941,.

18. Bakry A, Ahmed M. Harmonic and intermodulation distortions and noise associated with two-tone modulation of high-speed semiconductor lasers. Phys. Wave Phenomen. 2016;24:64-72.
19. Tartarini G, Lena A, Passaro D, Rosa l, Selleri S, Faccin P, Maria fabbri E. Harmonic and intermodulation distortion modeling in IM-DD multi-band radio over fiber links exploiting injection locked lasers. Opt. Quantum Electronic. 2006;38:869–876.
20. Lu HH, Lin YP, Lin MC. Nonlinear distortion analysis for directly modulated dfb laser diode in CATV systems. J. Opt. Commun. 2001;22:1-3.
21. Yamada H, Okuda T, Torikai T, Uji T. Dynamic L-I characteristics measurement of laser diodes for analyzing intermodulation distortion mechanism. Proc. 15th IEEE Intl. Conf. Semicond. Laser. 1997;177-178,.
22. Chrys Mendis FV, Haldar MK, Pang-Shyan Kooi, Jun Wang. Intermodulation distortion in semiconductor lasers in application to subcarrier multiplexed fiber optic video systems. Oopt. Eng. 1994;33: 2697.
23. KREHLIK P. Characterization of semiconductor laser frequency chirp based on signal distortion in dispersive optical fiber. OPTO-Electronics Review. 2006; 14(2):123 -128.
24. Cartledge JC, Burley GS. The effect of laser chirping on lightwave system performance. J. Lightwave Technol. 1989;7:568 - 573.
25. Ahmed M, Yamada M. Mode oscillation and harmonic distortions associated with sinusoidal modulation of semiconductor lasers. Europ. Phys. J. D. 2012;66:264-9.
26. Potasek MJ, Agrawa GP. Self-Amplitude modulation of Opticl pulses in nonlinear dispersive Fibers. Phys. Rev. A. 1998;35:3862.
27. Agrawal GP. Nonlinear Fiber Optics (Academic Press, San Diego, 2001).
28. Ahmed M, Ellafi A. Large-signal analysis of analog intensity modulation semiconductor lasers. Opt. and Laser Techn. 2008; 40:809-819.

Peer-review history:
The peer review history for this paper can be accessed here:
http://www.sdiarticle4.com/review-history/68313